

See discussions, stats, and author profiles for this publication at: <https://www.researchgate.net/publication/305220204>

Towards a Cavity Enhanced Thomson Scattering Diagnostic for Electric Propulsion Research

Conference Paper · October 2013

CITATIONS

2

READS

419

4 authors, including:



Adam J Friss

National Institute of Standards and Technology

16 PUBLICATIONS 66 CITATIONS

[SEE PROFILE](#)



Brian Lee

Takeda

7 PUBLICATIONS 22 CITATIONS

[SEE PROFILE](#)



Azer Yalin

Colorado State University

174 PUBLICATIONS 2,054 CITATIONS

[SEE PROFILE](#)

Some of the authors of this publication are also working on these related projects:



Study of ammonia deposition downwind of concentrated animal feeding operations (CAFOs) using unmanned aerial system (UAS) laser sensor [View project](#)



Cavity Enhanced Thomson Scattering [View project](#)

Towards a Cavity Enhanced Thomson Scattering Diagnostic for Electric Propulsion Research

IEPC-2013-351

*Presented at the 33rd International Electric Propulsion Conference,
The George Washington University • Washington, D.C. • USA
October 6 – 10, 2013*

Adam Friss¹, Brian Lee², Isaiah Franka³, and Azer Yalin⁴
Colorado State University, Fort Collins, CO, 80523, USA

We report on the development of a cavity enhanced Thomson scattering (CETS) diagnostic to measure electron density and temperature in weakly ionized discharges. The method uses an intra-cavity beam with average power several orders of magnitude greater than that of illumination sources typically used for Thomson scattering. The increase in illumination source power will yield stronger Thomson signals thereby improving diagnostic sensitivity and enabling measurements in weakly ionized discharges such as Hall thruster plasmas. Here, we focus on recent experimental progress towards the CETS diagnostic. We demonstrate locking of narrow linewidth 1064 nm fiber laser to a high finesse cavity (finesse $\approx 24,000$) and achieve a power build-up factor of 430. We also present characterization of a triple-pass monochromator and photomultiplier tube in photon counting mode and a demonstration of Rayleigh scattering from the ambient room air. Future steps to increase the intra-cavity power are discussed.

Nomenclature

| | | |
|----------------|---|---|
| C | = | Coupling factor of source laser to cavity |
| I_{cav} | = | Intra-cavity power |
| I_L | = | Power of source laser |
| n_e | = | Electron number density |
| R | = | Cavity mirror reflectivity |
| $EEDF$ | = | Electron energy distribution function |
| LTS | = | Laser Thomson scattering |
| σ_{Th} | = | Thomson scattering cross section |
| σ_{Ray} | = | Rayleigh scattering cross section |
| HR | = | High reflectivity |
| $CRDS$ | = | Cavity ring-down spectroscopy |
| F | = | Finesse |
| FSR | = | Free spectral range |
| NIR | = | Near infrared |
| AOM | = | Acousto-Optic Modulator |
| EOM | = | Electro-Optic Modulator |

I. Introduction

Electric propulsion (EP) systems have seen widespread use in applications including satellite station keeping and propulsion for deep space missions. Due to the ever-increasing demands of future applications, there is a focus on improving device performance (thrust, efficiency, lifetime), and improving the understanding of the physics that

¹ Graduate Student, Department of Mechanical Engineering, ajf787@rams.colostate.edu.

² PhD Candidate, Department of Physics, blee66@rams.colostate.edu.

³ Research Engineer, Seaforth LLC, ifranka@rams.colostate.edu.

⁴ Associate Professor, Department of Mechanical Engineering, ayalin@engr.colostate.edu.

govern EP systems. In particular, current work on the development of high-power long-life Hall thrusters requires a more fundamental understanding of plasma characteristics. Electrons play a key role in these devices in terms of controlling ionization and energy coupling, and ultimately the channel impedance and thruster efficiency; however available electron diagnostics are limited. To aid in the development of physics-based models of plasma, the capabilities for measuring electron number density (n_e) and electron energy distribution function (EEDF) must be improved. Laser Thomson Scattering (LTS) is one of the few non-intrusive electron diagnostics; however, challenges of low signal levels and optical interference place limits on the applicability of the technique¹. The overall goal of the present research is to develop a new means of Thomson scattering, based on the use of a high power intra-cavity beam as the light source, which will allow for more widespread use of LTS in EP research.

Despite the attractive nature of LTS, several challenges limit the use and applicability of the technique¹⁻³. The primary challenge in LTS is small scattering cross-sections, (integrated cross-section of $\sigma_{Th}=6.65 \times 10^{-29} \text{ m}^2$) so signal levels are extremely weak. In order to obtain usable signal levels, typical experiments employ relatively high power pulsed lasers, e.g. Q-switched Nd:YAG lasers with pulse energies of $\sim 0.1\text{-}1 \text{ J}$ and repetition rates of $\sim 10\text{-}100 \text{ Hz}$ (average power of $\sim 1\text{-}100 \text{ W}$)²⁻⁴. Other challenges include the need to suppress Rayleigh and elastic scattered light (spectrally positioned at the center of the LTS lineshape), and in some cases, light from nearby optical emission lines, for which multi-pass spectrometers are typically used²⁻⁴ and vapor filters have also been demonstrated⁵. Even when these methods are employed, sensitive measurements are difficult. Measurement durations (to study one plasma condition) are often many tens of minutes with measurements in the range of $n_e \sim 10^{11}\text{-}10^{12} \text{ cm}^{-3}$ being considered challenging to state-of-the-art².

The new approach, which we term cavity-enhanced Thomson scattering (CETS), aims to capitalize on the high power of an intra-cavity beam, i.e. a beam whose power builds up within a high-finesse optical cavity. We intend to produce an intra-cavity beam of power $\sim 10\text{-}100 \text{ kW}$ or higher, which is several orders of magnitude higher than average powers conventionally used, thereby resulting in higher counts of Thomson scattered photons (for a given measurement time). Relative to the use of pulsed lasers, where the high peak powers can perturb the plasma species populations (e.g. Ref. 4), the lower peak powers proposed here should have reduced effect on the plasma. The technique will have high spatial resolution and, by repeated phase-locked measurements of periodic events, temporal resolution should also be possible so that dynamic processes such as the Hall thruster breathing mode can be studied. On the other hand, the continuous nature of the light collection means that interfering luminosity (for example from broadband emission) may be more problematic; if needed, techniques such as chopping and phase-sensitive detection can be used. Past Thomson experiments have used Herriot or multi-pass cells to provide a modest increase in the effective power of a pulsed laser^{3,6}. The use of continuous-wave intra-cavity beams for scattering diagnostics has been reported in the past for Rayleigh and Raman scattering⁷ though the powers obtained in those cases were orders of magnitude lower than we will attain. The higher powers in our work will be achieved by capitalizing on recent advances in several optical components including narrow linewidth high power fiber laser sources, ultralow-loss mirrors, and increasingly available laser locking hardware. Improved Rayleigh- and Raman-scattering measurements, both by rotational and vibrational Raman, should also be enabled with similar instrument configurations.

The CETS diagnostic technique has been introduced in our past work^{8,9}. In summary, a narrow linewidth laser source is coupled to a linear cavity formed from two high-reflectivity (HR) mirrors. Such mirrors, sometimes termed super-mirrors, are based on quarter-wave dielectric layers and are widely used in cavity-enhanced techniques (e.g. cavity ring-down spectroscopy¹⁰) due to the availability of reflectivities in excess of 99.99% over many spectral regions. The laser and cavity frequencies are locked together with the Pound-Drever-Hall (PDH) locking technique, which results in a large buildup of intra-cavity power. The high intra-cavity power serves as the light source for Thomson scattering, and the plasma to be studied is housed within the cavity. The Thomson-scattered light is collected by a lens (nominally) orthogonal to the cavity and focused into a triple-monochromator and detector. Our initial setup employs a photomultiplier tube (PMT) though array detectors can also be considered. Thomson scattering is a non-resonant phenomenon with cross-section independent of wavelength. The CETS system has been developed using a near-infrared (NIR) narrow linewidth ytterbium (Yb) fiber laser at 1064 nm (details in Sec. IIA). The light source was selected owing to its commercial availability and attractive NIR operation in terms of avoiding plasma emission lines, which tend to be more prevalent in the visible and ultraviolet, and improved ratio of Thomson to (competing) Rayleigh scattering cross-sections ($\sigma_{Ray} \propto \lambda^{-4}$). However, a drawback of NIR operation relative to visible or ultraviolet wavelengths is that photo-detectors typically have lower quantum efficiency.

The intra-cavity power achieved by injecting a laser beam into an optical is given by,

$$I_{cav} = \frac{CI_L}{2(1-R)} \quad (1)$$

where I_{cav} is the intra-cavity power, I_L is the power of the source laser, R is the mirror reflectivity, and C is a coupling factor¹¹. Efficient coupling in the spatial domain requires mode-matching¹² of a near single-mode source, i.e. a beam that is near TEM₀₀ (or $M^2=1$), to the optical cavity as is done in CRDS and related cavity enhanced techniques. The coupling factor would approach unity if the laser were perfectly matched to the cavity in the spatial and frequency domains¹¹ and would result in an enhancement factor (ratio of intra-cavity to incident laser power) approaching $1/(1-R)$ (e.g. enhancements approaching 10,000 for mirrors with $R=0.9999$). The enhancement factor closely relates to cavity finesse which, in the limit of high-reflectivity mirrors, can be approximated as $F=\pi/(1-R)$. As the cavity finesse increases, the spectral width of the cavity transmission peaks narrows and therefore, efficient frequency coupling requires narrow linewidth laser sources (\sim kHz for typical cavity lengths of \sim 1 m and finesse of $>10,000$) such as a single-mode fiber laser. Of course, efficient power coupling also requires the laser and cavity frequencies to be overlapped, so therefore a locking technique should be used. Owing to the commercial availability of high-bandwidth modules¹³, sharp error signal, and relative insensitivity to laser intensity fluctuations, the PDH technique was selected for our setup (see Section IIB).

Further details of the diagnostic approach, including experimental setup, are presented in Section II. CETS results are presented in Section III, which include initial experimental results, such as cavity locking, detection system characterization, and Rayleigh scattering measurements. Finally, conclusions are presented in Section IV.

II. Experimental Setup

The CETS setup is divided into four main categories: laser and optical cavity (Section IIA), locking optics and electronics (Section IIB), scattering detection (Section IIC), and future implementation of a double-pass acousto-optic modulator (AOM) with a cat's eye retro-reflector for fast laser-frequency feedback (Section IID). The initial setup has been used for proof of concept studies including demonstrations of cavity locking, instrument characterization, and Rayleigh scattering. Initial studies are performed with a 40 mW laser and cavity with finesse of $F\approx 24,000$, though future development will strive to lock higher finesse cavities of $F>100,000$ and will use a higher power 5 W source.

A. Laser and Optical Cavity

The instrument configuration is shown in Fig. 1. A single-mode fiber laser (SI-2000 Continuum) operating at 1064 nm serves as a narrow linewidth source with power of \sim 40 mW and linewidth <5 kHz. An optical isolator prevents reflected light from propagating back into the laser. Mode-matching of the beam to the cavity is performed with the use of an aspheric lens mounted on a translation stage at the fiber output of the laser. The optical cavity, formed with two HR mirrors, is approximately 50 cm in length. The first cavity mirror (M1) is flat and is mounted to a piezo-actuator to allow for modulation of the cavity length. The second cavity mirror (M2) has a radius of curvature of 1 m. Practical concerns related to maintaining high mirror reflectivity and continuous cavity locking with the high power beam and plasma present inside the optical cavity were discussed in our past work⁸ and will not be covered here.

The optical cavity and its alignment were characterized. An AOM (IntraAction, ATM-803DA6B) acts as an optical switch allowing fast extinction (\sim 250 ns) of light injection to the cavity, allowing measurement of the exponential decay of light within the cavity, i.e. cavity ring-down signal¹⁰, from which the mirror reflectivity and cavity finesse can be determined. We find a ring-down time of 12.99 μ s, corresponding to $R=0.99987$ (consistent with manufacturer's specification of $R>0.9997$) and finesse of 24,000. Confirmation and optimization of the spatial mode-match, i.e. that the TEM₀₀ mode is predominantly coupled to the cavity (see Section IIIA), is performed by monitoring the transmission signal as the cavity length is scanned using the piezo-actuator.

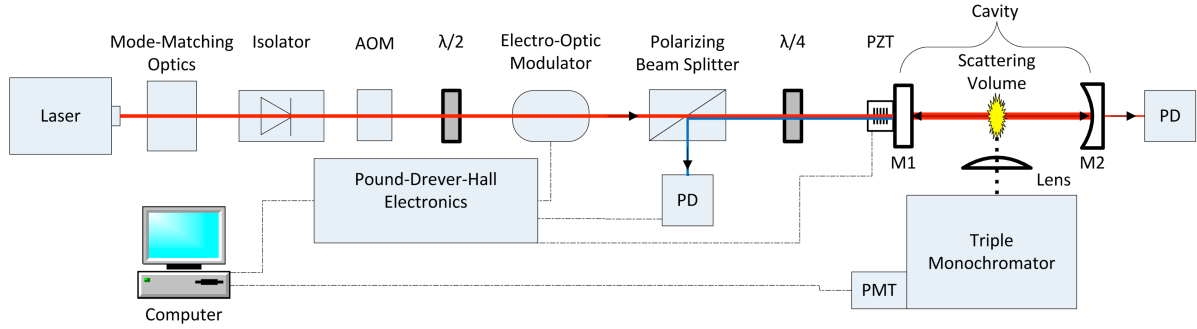


Figure 1. Schematic diagram of cavity-enhanced Thomson scattering setup. A high-finesse optical cavity is frequency locked to a narrow-linewidth laser source using the Pound-Drever-Hall technique. The resulting high power intra-cavity beam is the light source for Thomson scattering and the plasma under investigation (labeled scattering volume) is housed within the optical cavity. The scattering signal is collected by a lens and dispersed by a triple monochromator. The inclusion of an acousto-optic modulator also allows cavity ring-down measurements to assess finesse.

B. Cavity Locking

Optical locking of the cavity resonance frequency to the laser frequency, as is needed to build up high power within the cavity, is accomplished with the use of a commercially available electro-optic modulator (EOM) and PDH locking module (Toptica Photonics, Digilock 110). The electro-optic modulator (Photonics Technologies, EOM-01-12.5-IR) is used to generate sidebands at ± 12.5 MHz relative to the center laser frequency. The locking module provides the modulation signal to the EOM, monitors the cavity reflected intensity, which is used to internally generate the PDH error signal, and to control the piezo-actuator on the cavity mirror in order to maintain frequency locking. Note that the fiber laser we use cannot accept feedback, though for some other source (current or thermal) feedback to the laser could also be used. The error signal is derived from the light reflected from the input cavity mirror, which is picked out of the beam line using a polarizing beam cube and quarter wave-plate, and measured with a 35-MHz bandwidth photodiode (Thor Labs, DET10C). The PDH locking module is capable of a bandwidth approaching 20 MHz while the piezo-actuator scan module (Toptica Photonics, SC110) has a bandwidth of 10 kHz. However, initial tuning of the piezo feedback PID loop indicates a bandwidth limit of 5 kHz in the current instrument configuration, likely due to the mass and capacitance of the piezo and mirror. With further optimization the upper limit of 10 kHz due to the scan module should be achievable (see also Section IID).

In order to characterize the locking bandwidth requirements, the extent and bandwidth of the frequency drift of the cavity (e.g. due to acoustic noise, mechanical vibrations, laser frequency drift, as well as the presence of plasma or combustion within the cavity) needs to be understood. If one assumes that the laser frequency is constant, the cavity frequency drift can be studied by scanning the cavity length and then measuring (in the time domain) the position and movement of the cavity resonance peaks, which is accomplished by looking at the cavity transmission signal with a photodiode (New Focus, 2053-FS). Extensive research has been performed on cavity design and isolation to minimize sources of drift, for example to develop narrow linewidth lasers. A common design utilizes ultralow expansion glass, vertical mounting, and monolithic supports¹⁴. Further stabilization can be achieved by maintaining a steady state temperature and with vibration isolation via floating optical tables and damping systems. However, we aim to design a robust and practical diagnostic for plasma and combustion environments that has suitable optical access and can be used in the presence of mechanical sources of noise (e.g. vacuum chamber pumps and equipment) typically present during plasma source operation and are therefore reluctant to adopt such approaches. The initial CETS cavity is comprised of two half-inch low-drift mirror mounts (ThorLabs, Polaris-K05) bolted directly to a 2" x 2" length of 6061 aluminum bar stock mounted to an optical table via 1" diameter optical posts. Additionally, a length of rigid tubing has been placed between the two cavity mirrors to reduce the negative effects of air currents and to prevent any scattered intra-cavity power from becoming a safety hazard. The current cavity design would obstruct diagnostics, but serves as a proof of concept and can likely be modified in the future to allow needed optical access.

Detailed stability studies have been performed and were discussed in our previous work⁹. In summary, it was found that to achieve and maintain a lock, the extent of the frequency drift of the cavity must be less than what can be compensated for by the piezo-actuator. The physical displacement of the actuator (measured experimentally) is

currently limited by the scan control module to approximately 436 nm, which corresponds to 82% of one cavity free spectral range (FSR). If the cavity drift, i.e. drift in cavity transmission peak location, exceeds the range of the actuator, the lock will be lost, at least temporarily. Similarly, if the cavity resonance location varies at a frequency greater than the 10 kHz bandwidth limit, the lock will be lost. On the timescale of a few seconds, the transmission peak location drifted by less than one percent of an FSR, well under the ~ 0.82 FSR that can be corrected by the locking system. Over timescales of minutes the location is within the range of the actuator; however, excessive mechanical or acoustic perturbations cause the location to drift beyond the range over which the actuator can compensate. Sampling of the transmission location was restricted to hundreds of hertz due to actuator limitations and therefore no conclusions can be drawn in regards to sources of noise faster than the sampling rate.

C. Scattering Detection

Detection of scattered signals employs a triple-monochromator (SPEX-1877) for dispersion of the signal in conjunction with a near infrared (NIR) photomultiplier tube (PMT) (Hamamatsu, H10330B) and a multichannel scaler (Stanford Research Systems, SR430) for photon counting. The triple-monochromator is selected owing to its strong suppression characteristics (specified by the manufacturer as 10^{14} at 10 bandpass units from line center). The high suppression achievable with this triple-monochromator is necessary to discern the Thomson and rotational Raman signal against the strong Rayleigh and background signals. As shown in Fig. 2, the monochromator is comprised of two main sections. The first stage (in blue, S1-M5) acts as a wavelength-selectable bandpass as it consists of a 0.22 m double monochromator with gratings (G1 & G2) locked in subtractive-dispersion mode. The non-dispersed light from the filter stage is then directed into a 0.6 m single monochromator known as the spectrograph stage (in red, S3-M8), which disperses the light over the detector. Instrument suppression characteristics have been examined and will be discussed in Section IIIB. For operation at 1064 nm (outside the regular range), the three gratings were replaced with low-stray light gratings (Richardson, 53009BK01-520R) that allow operation in the NIR wavelength region. Based on mirror and grating efficiency measurements from the manufacturer, approximately 22% of the 1064-nm light should reach the output detector (assuming no slit loss). Calibration of the wavelength axis and absolute signal levels can be accomplished via rotational Raman scattering, i.e. one can measure the scattering spectrum due to N_2 or O_2 (or other species with known rotational constants and rotational Raman cross-sections) and scale the axes accordingly¹⁵.

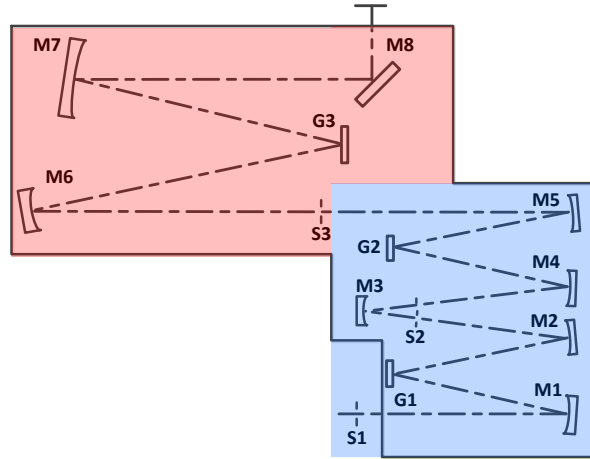


Figure 2. SPEX-1877 Triple-monochromator. High suppression is accomplished with two stages: wavelength selectable bandpass stage (blue) and a spectrograph stage (pink). Internal mirrors (M), gratings (G), and entrance and beam block slits (S) are shown with the beam path designated by the dashed line.

D. Double-pass AOM

The current setup for locking the cavity to the laser (Section IIA) involves adjusting the cavity length via a piezo-actuator to maintain spectral overlap between the laser and cavity frequencies. A lock can be maintained for extended periods of time by adjusting the cavity length rapidly, but noise with higher frequency than the bandwidth of the actuator cannot be compensated for and manifests as power fluctuations within the cavity (measured by monitoring cavity transmission) or in extreme cases, as a loss of lock. With improved PID parameters and further

laser and cavity stabilization some of the faster sources of noise can be reduced, but ultimately it will be beneficial to have improved bandwidth (speed) in our locking circuit. The bandwidth of the piezo-actuator feedback loop can be somewhat improved but is fundamentally limited to kHz rates by the mass and capacitance of the piezo-mirror.

One method, which we aim to implement, to provide faster feedback (increased bandwidth) would be to use an AOM to shift the frequency of the laser. As a beam of frequency ω passes through an AOM operating at a modulation frequency Ω , (Fig. 3a) the frequency is shifted to $\omega + \Omega$. Acousto-optic modulators typically operate at tens of MHz and therefore induce a sufficient frequency shift to help maintain the spectral overlap of the cavity and laser frequencies, thus improving the lock. Additionally, because AOM's have a rise time on the order of tens to hundreds of ns, a frequency shift bandwidth of several MHz is readily achievable. Therefore, by using the AOM to provide fast feedback, it is possible to suppress fast environmental and system noise while using the slower piezo loop to combat slower sources of noise (e.g. thermal drift of the cavity, low frequency mechanical vibrations, etc.). The PDH module is designed to drive two PID loops: a fast loop to drive the AOM with a bandwidth upper limit of 19 MHz and a slow loop currently limited by the SC110 module to 10 kHz. Implementation of a fast loop will allow significant improvements in the instrument's ability to maintain a high quality lock.

The diffraction angle of the first (and higher) order beam(s) produced with an AOM is dependent on the modulation frequency. Thus, as the laser frequency is scanned via the AOM, the diffraction angle shifts, and the position of the beam in relation to the cavity changes, which for use with a resonant cavity, is undesirable as alignment is crucial to maintain resonance and a lock. A common method to eliminate the angular dependence on modulation frequency is to use a double-pass configuration in which the beam is retro-reflected back through the AOM resulting in an additional frequency shift of Ω and a beam that exits along the input beam path independent of modulation frequency¹⁶. Such a technique is frequently referred to as a "cat's-eye configuration." Figure 3b depicts a basic cat's-eye double-pass AOM setup. In essence, a beam is directed through an AOM followed by a lens placed a distance away from the AOM equal to its focal length. Regardless of the diffraction angle of the beam all the rays emanate from the focal point of the lens and are parallel to the zero order beam. Therefore, with careful alignment, a mirror (M) can be set such that all rays strike it at normal incidence and are retro-reflected back along the incoming beam path allowing cavity alignment to be maintained regardless of AOM modulation frequency. By using linearly polarized light, a polarizing beam splitter (PBS), and a quarter wave plate (QWP), light exiting the AOM on the second pass is polarized orthogonal to the input beam and is then picked out of the beam line with the PBS and directed to the cavity.

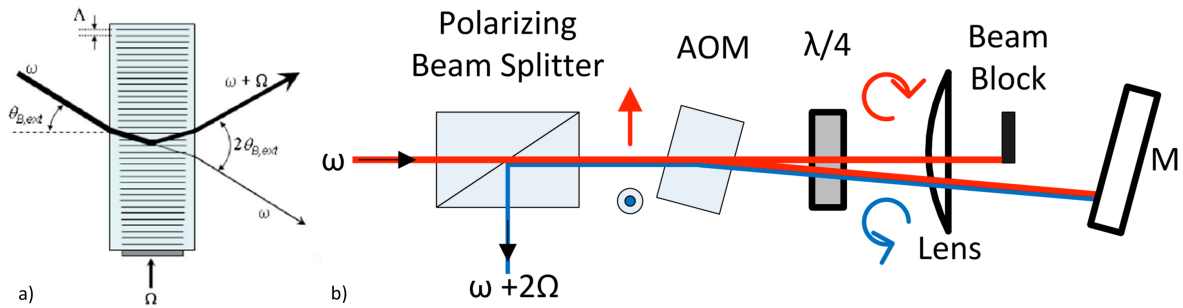


Figure 3. Double-pass AOM Setup. a.) Schematic diagram of an AOM operating at a modulation frequency Ω . The incident laser beam is at a frequency ω and first order diffracted beam is shifted to a frequency of $\omega + \Omega$.¹⁶ b.) Double-pass AOM system where the beam enters in red at frequency ω and exits in blue at frequency $\omega + 2\Omega$. Polarization is show by red and blue arrows. Beams have been offset and angles exaggerated for display purposes.

III. Results and Discussion

A. Cavity Locking

Optimum coupling in the spatial domain of the laser to the cavity requires mode-matching of a near single mode beam to the cavity (i.e. TEM₀₀). Mode-matching, as discussed in Section IIA, is achieved with an aspheric lens. To verify the quality of the mode-match, transmitted intensity is monitored as the cavity is scanned. If the cavity were strongly coupled to only the TEM₀₀ mode, all the transmission peaks would be regularly spaced by the cavity FSR. Because the translation of the actuator is limited to ~246 MHz, it is difficult to assess the quality of the mode-match

in this way. However, even while scanning less than one FSR, it is apparent more than one mode is present (Fig. 4a). Based only on cavity transmission, it is not possible to tell which mode is the TEM_{00} . To ensure the cavity is locked to the correct mode, the output of the locked cavity was imaged with a CCD. Figure 4b shows a zoomed in view of Fig. 4a and the TEM_{00} mode has been labeled. Laser sidebands can be observed at ± 12.5 MHz. The higher order mode was determined to be the TEM_{01} mode based on the CCD image and relative frequency spacing of 75 MHz. In practice, it is very difficult to have all power in the TEM_{00} mode; our current setup has about 70% of the power in the mode which we aim to increase to $\sim 90\%$ by improving the mode-matching optics and alignment.

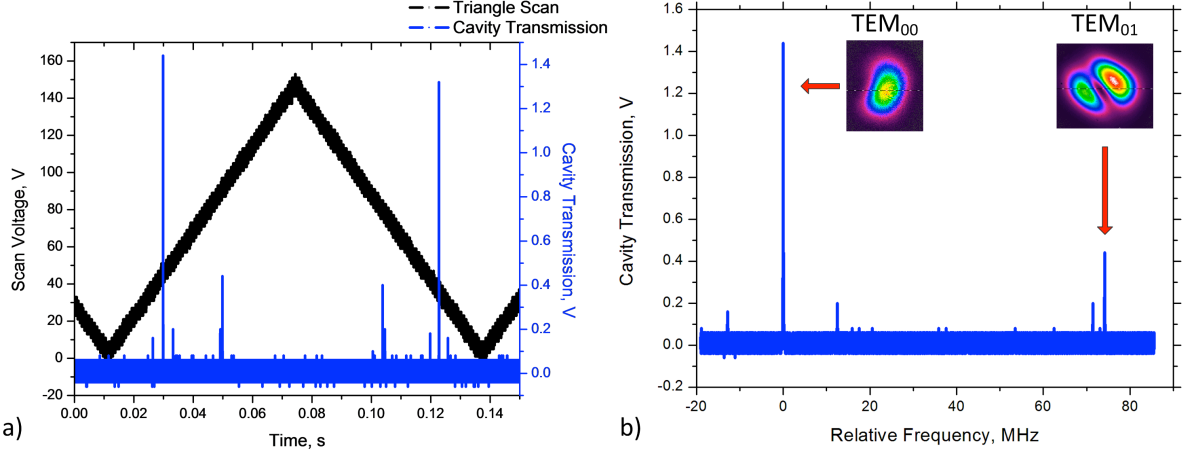


Figure 4. Mode-Match. *a).* As a triangle scan is applied to the actuator (black), cavity transmission (blue) is monitored with a photo diode. *b).* Zoomed in view of mode structure with TEM_{00} located at 0 MHz and TEM_{01} located at 75 MHz.

We have demonstrated locking of the cavity as is shown in Figs. 5a and 5b, which depicts the cavity transmission signal (measured with a photodiode behind cavity) over a duration of ~ 8 ms and 16 s respectively. In the absence of locking, one would have nominally zero transmission with, perhaps, some intermittent signal due to random coincidences of laser and cavity frequency caused by drift. With the lock engaged, one observes a significantly higher average transmitted power that is always above “zero” due to the overlapped cavity and laser frequencies. The laser and cavity linewidths are < 5 kHz and 20 kHz, respectively. An ideal lock would involve perfect coupling of the cavity to the laser and thus a spectral overlap of the lineshapes. However, because the lineshapes are so narrow even small perturbations of the cavity frequency due to noise can cause a significant drop in coupling efficiency. The locked transmission signal is somewhat noisy and should be improvable with fine-tuning of the PID loop that drives the mirror actuator. Ultimately though, the actuator will reach a bandwidth limit above which no improvement can be made. Work in this area is ongoing and future implementation of a double-pass AOM (Sec. IID) should allow significant improvements in lock quality by providing a feedback mechanism to combat noise above the bandwidth of the actuator. Despite less than ideal locking, we have been able to maintain the lock for several minutes even with a turbo pump, roughing pump, and various other sources of mechanical vibrations running on the same optical table.

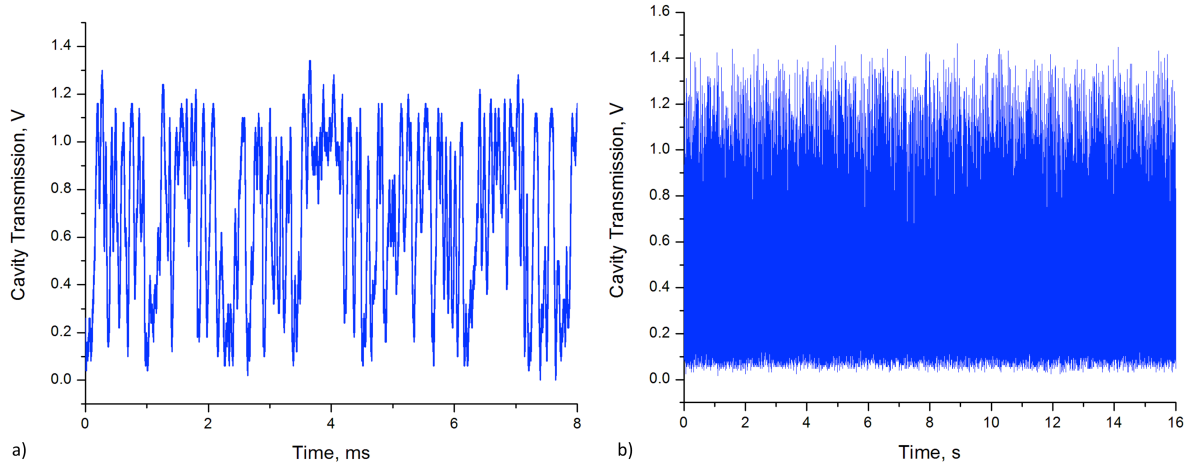


Figure 5. *a,b) Measured cavity transmission with the PDH lock engaged. A time-averaged transmitted power of 0.25 mW was measured, corresponding to ~ 4 W intra-cavity power.*

Intra-cavity power can be estimated based on the incident and transmitted laser power. An incident power of 9 mW and transmitted power of 0.25 mW was measured with a power meter (Coherent Inc., Field Mate). Based on these measurements, the intra-cavity power is estimated to be approximately 3.9 W. As mentioned above, a mirror reflectivity of $R=0.99987$ was measured, and should theoretically correspond to a power build factor of ≈ 7700 , which would result in an intra-cavity power of 35 W. Therefore, the current setup is operating with coupling efficiency of $C \approx 0.1$ and a build-up factor of ≈ 430 .

B. Detection System Characterization

The ultimate goal of CETS is to measure n_e and EEDF via Thomson scattering in weakly ionized plasmas such as electric propulsion devices. Because the Thomson signal is so weak in comparison to other spectrally overlapped and competing phenomena, a high degree of suppression is required for CETS. High spectral dispersion is achieved with a triple-monochromator. To assess instrument broadening, the laser source (<5 kHz line width) was scattered off of a card, and some of the scattered light was collected and focused into the triple monochromator. These measurements were performed for initial slit widths of 300 μm though these values may be adjusted and optimized in future work. Figure 6 depicts the measured transmitted line shape of the scatter light. The transmitted light has a FWHM of approximately 1 nm. At this level of resolution, it would be possible to perform Rayleigh and Thomson scattering but would present significant difficulties in resolving Raman spectra. The broadening of the monochromator can be reduced by improving alignment on the entrance slit and by reducing the slit widths. In the future, these parameters will be optimized and the suppression away from line center characterized.

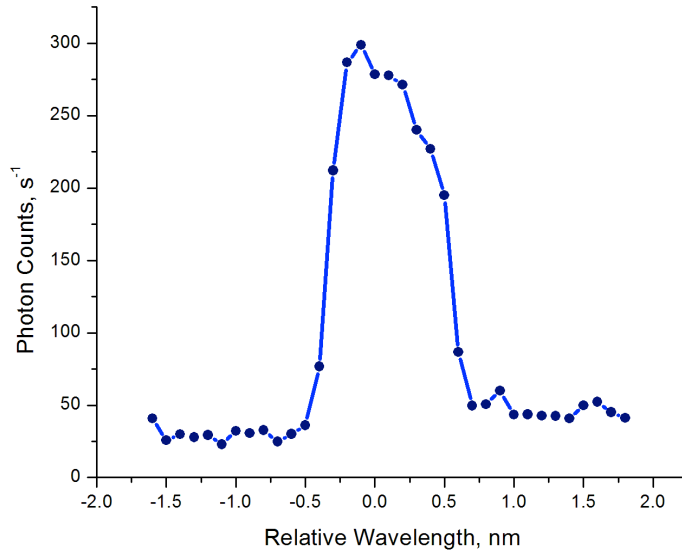


Figure 6. Instrument function of the SPEX-1877 Triple-monochromator. *Photon counts are plotted versus wavelength for (narrowband) scattered light centered at 1064 nm. The instrument function lineshape has a 1 nm FWHM indicating instrument broadening.*

C. Rayleigh Scattering

Initial Rayleigh scattering measurements of ambient laboratory air have been performed by collecting scattered light from the locked cavity (power ~ 4 W) into the triple-monochromator. All collection was performed orthogonal to the cavity. A 10 cm focal length (f) lens was placed a distance f away from the cavity. The collected light was then aligned (using a periscope) with a second 10 cm focal length lens, which was mounted in a translation stage to allow for precise positioning of the lens a distance f away from the monochromator entrance slit. Both the entrance and exit slits were set to 300 μm . Significant effort was taken to ensure there was minimal laser scatter from optics, which would have overpowered the Rayleigh signal. We have verified the signal was due to Rayleigh scattering (as opposed to other elastic scatter) by blocking the beam at various locations. Figure 7 shows the measured Rayleigh signal, which has been broadened to $\text{FWHM} \approx 1$ nm due to the instrument function, versus photon counts per second. Photon counting was performed with a multichannel scaler with a temporal bin width of 163.84 μs per bin and 10^5 bins per scan resulting in a collection time of 16.384 seconds per data point. The number of detected counts was low, nonetheless it is noteworthy to detect Rayleigh scattering from light generated by a near-infrared milliwatt diode laser. Moving to a higher-power source, or improving the quality of the lock and coupling of the laser to the cavity, would result in a much stronger Rayleigh signal and therefore higher photon counts.

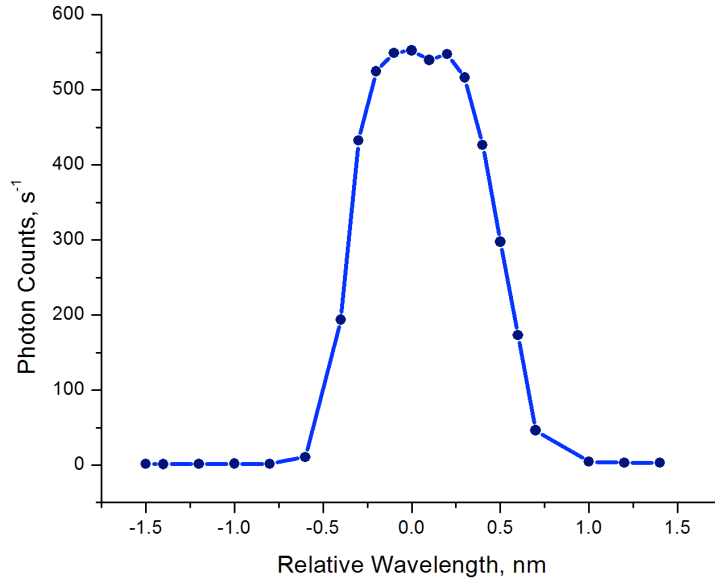


Figure 7. Detection of Rayleigh scattering from laboratory air. The CETS instrument was used to generate an intra-cavity power of ≈ 4 W, which acted as the illumination source for scattering measurements.

IV. Conclusion

The novel CETS approach appears promising for spatially- and temporally-resolved measurements of low electron densities in low temperature discharges. The system capitalizes on the high photon counts provided by a high power intra-cavity beam and is enabled by recent technological developments in the areas of high-reflectivity mirrors, narrow linewidth high-power fiber lasers, and locking modules. We have demonstrated locking, even in the presence of vibration and noise from nearby mechanical pumps, for periods of several minutes, which is promising for future work in which we will have perturbations from plasma or combustion. We employed a cavity finesse of 24,000 for which we obtained an estimated intra-cavity power of 3.85 W. Initial Rayleigh scattering measurements have been presented. The path towards higher kW level intra-cavity power includes the use of a 5 W (as opposed to 40 mW) source, and improving the bandwidth and fidelity of the locking. If improved locking is achieved, we can then attempt the use of higher reflectivity mirrors. In addition to locking challenges, other potential challenges when studying plasma include index-of-refraction variations within the cavity as well as possible chemical etching, ultraviolet exposure, potential electron heating, and particulate deposition on the cavity mirrors as has been discussed in our past work⁸. However, successful cavity ring-down measurements in plasmas (with long decay times in the range of ~ 100 μ s) support the viability of maintain high cavity finesse in the presence of plasmas^{17,18}. Additional challenges will be present in the light collection leg including Rayleigh and background suppression, as well as mitigation of optical emission (line and broadband), which will be more difficult for our c-w system as compared to past work with pulsed sources where temporal gating can be used. If we can be successful, the payoff will be high as we will expand the applicability of Thomson scattering to allow measurements in many weakly ionized discharges including EP plasmas.

References

- ¹ Hutchinson, I. H., *Principles of Plasma Diagnostics*, Cambridge: Cambridge University Press, 2005.
- ² Muraoka, K., and Kono, A., "Laser Thomson scattering for low-temperature plasmas," *Journal of Physics D: Applied Physics*, vol. 44, Feb. 2011, p. 043001.

- 3 Bowden, M. D., Goto, Y., Yanaga, H., Howarth, P. J. A., Uchino, K., and Muraoka, K., "A Thomson scattering diagnostic system for measurement of electron properties of processing plasmas," *Plasma Sources Science and Technology*, vol. 8, 1999, pp. 203–209.
- 4 Yamamoto, N., Tomita, K., Sugita, K., Kurita, T., Nakashima, H., and Uchino, K., "Measurement of xenon plasma properties in an ion thruster using laser Thomson scattering technique.," *The Review of scientific instruments*, vol. 83, Jul. 2012, p. 073106.
- 5 Zaidi, S. H., Tang, Z., Yalin, A. P., and Miles, R. B., "Filtered Thomson scattering in an argon plasma," *AIAA Journal*(0001-1452 ..., vol. 40, 2002, pp. 1087–1093.
- 6 Kantor, M. Y., Donné, a J. H., Jaspers, R., and van der Meiden, H. J., "Thomson scattering system on the TEXTOR tokamak using a multi-pass laser beam configuration," *Plasma Physics and Controlled Fusion*, vol. 51, May. 2009, p. 055002.
- 7 Hercher, M., Mueller, W., Klainer, S., Adamowicz, R. F., Meyers, R. E., and Schwartz, S. E., "An Efficient Intracavity Laser Raman Spectrometer," *Applied Spectroscopy*, vol. 32, May. 1978, pp. 298–302.
- 8 Wilvert, N., Joshi, S., and Yalin, A. P., "Ultraviolet Laser Plasma Preionization and Novel Thomson Scattering Method for Weakly Ionized Discharges," *AIAA 51st Aerospace Sciences Conference*, 2013, pp. 1–15.
- 9 Friss, A., Lee, B., Franka, I., and Yalin, A. P., "Cavity Enhanced Thomson Scattering for Diagnostics of Weakly Ionized Discharges," *44th AIAA Plasmadynamics and Lasers Conference*, 2013, pp. 1–9.
- 10 Berden, G., Peeters, R., and Meijer, G., "Cavity ring-down spectroscopy: experimental schemes and applications," *International Reviews in Physical ...*, vol. 19, 2000, pp. 565–507.
- 11 Paul, J. B., Lapson, L., and Anderson, J. G., "Ultrasensitive absorption spectroscopy with a high-finesse optical cavity and off-axis alignment," *Applied optics*, vol. 40, Sep. 2001, pp. 4904–10.
- 12 Kogelnik, H., and Li, T., "Laser beams and resonators," *Proceedings of the IEEE*, vol. 5, 1966, pp. 1550–1567.
- 13 Zhao, Y. N., Zhang, J., Stuhler, J., Schuricht, G., Lison, F., Lu, Z. H., and Wang, L. J., "Sub-Hertz frequency stabilization of a commercial diode laser," *Optics Communications*, vol. 283, Dec. 2010, pp. 4696–4700.
- 14 Ludlow, a D., Huang, X., Notcutt, M., Zanon-Willette, T., Foreman, S. M., Boyd, M. M., Blatt, S., and Ye, J., "Compact, thermal-noise-limited optical cavity for diode laser stabilization at 1×10^{-15} s," *Optics letters*, vol. 32, Mar. 2007, pp. 641–3.
- 15 Howard, J., James, B., and Smith, W. I. B., "Rotational Raman calibration of Thomson scattering," *Journal of Physics D: Applied ...*, vol. 1435, 1979.
- 16 Donley, E. a., Heavner, T. P., Levi, F., Tataw, M. O., and Jefferts, S. R., "Double-pass acousto-optic modulator system," *Review of Scientific Instruments*, vol. 76, 2005, p. 063112.
- 17 Yalin, A. P., Laux, C. O., Kruger, C. H., and Zare, R. N., "Spatial profiles of N₂⁺ concentration in an atmospheric pressure nitrogen glow discharge," *Plasma Sources Science ...*, vol. 11, 2002, pp. 248–253.

Hejduk, M., Dohnal, P., Varju, J., Rubovič, P., Plašil, R., and Glosík, J., “Nuclear spin state-resolved cavity ring-down spectroscopy diagnostics of a low-temperature H₃⁺ dominated plasma,” *Plasma Sources Science and Technology*, vol. 21, Apr. 2012, p. 024002.